Korean Grid Analysis Series 2025

KPG Platform Comparison Report

Advanced Grid Modeling Center

Korea Institute of Energy Technology

March 20, 2026

Abstract. This document is a technical report that summarizes the comparison results for the KPG Platform based on KPG193. To examine the numerical reliability and reproducibility of KPG Run, the report organizes the comparison procedures and results against PLEXOS, PSS/E, UnitCommitment.jl, and PowerModels.jl. In the comparisons with UnitCommitment.jl and PowerModels.jl, a high level of numerical consistency was confirmed for UC, DCOPF, and ACOPF. In the comparisons with PSS/E and PLEXOS, differences were observed depending on the modeling approach and simulation conditions.

1. Background

The Advanced Grid Modeling Center (AGM Center) is a research center that supports Korea's energy transition through open-source power-system modeling and stakeholder collaboration. To address technical and institutional challenges in the power-system and electricity-market domains, the AGM Center promotes reproducible open-source modeling, collaboration among stakeholders, and practitioner-oriented training. The integrated platform that embodies this research and collaboration agenda is the Korean Power Grid (KPG) Platform (**Figure 1**).

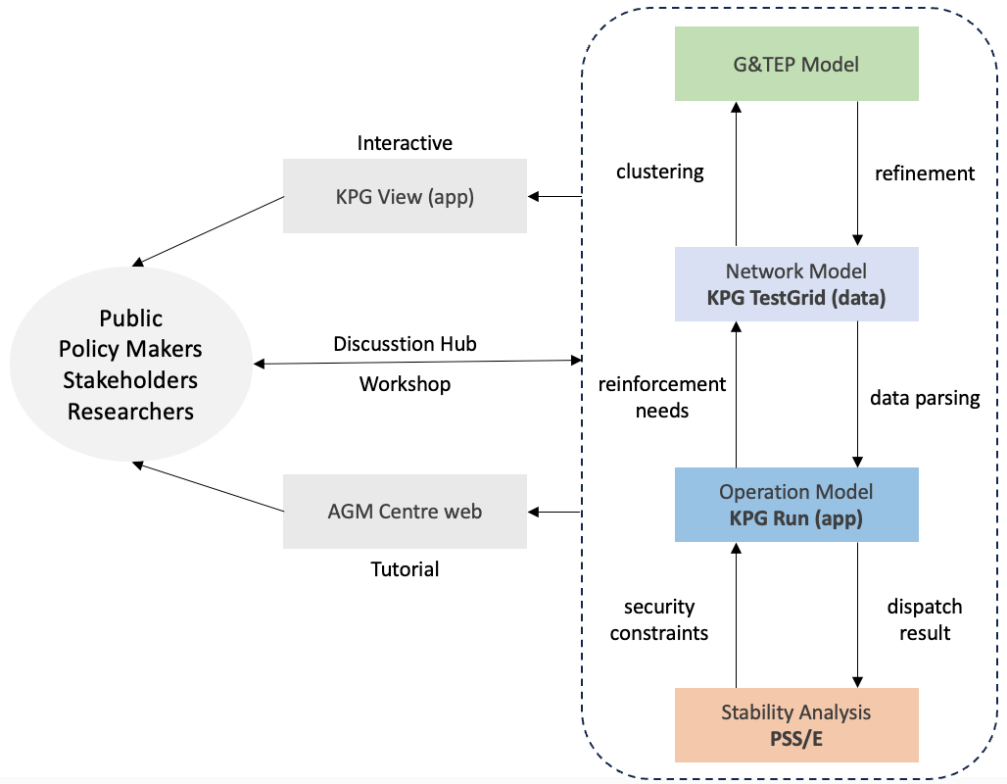

Figure 1. Overview and structural diagram of the KPG Platform

Platform component	Role
KPG TestGrid	A virtual Korean power-grid test system developed using only publicly available data.
KPG Run	A program that performs generation scheduling tasks such as unit commitment and optimal power flow.
KPG View	A visualization program for generation-scheduling results and power flow.
AGM Center Website	A web platform that introduces the AGM Center's major activities and online training programs, and provides downloads and user guides for KPG TestGrid, KPG Run, and KPG View. It is available at the following link: https://agm.kentech.ac.kr/.

Table 1. Major components of the KPG Platform and their roles

The main components of the KPG Platform and their roles are summarized in **Table 1**. At present, the AGM Center Website distributes KPG TestGrid, KPG Run, and KPG View, and supports generation-scheduling simulation and visualization for the virtual Korean transmission test system.

Conventional power-system analysis and generation-scheduling tools have long been used for large-scale system studies and the formulation of diverse operating plans. However, commercial software often does not fully disclose its internal model structure and data-processing workflow to users, and even open-source software has had limitations in consistently providing a reproducible research environment focused on the Korean power system. In contrast, the KPG Platform aims to provide a transparent and reproducible workflow for analyzing the Korean power system based on openly shareable data and open-source model implementations.

In particular, the KPG Platform links test-system construction (KPG TestGrid), generation-scheduling simulation (KPG Run), result interpretation and visualization (KPG View), and dissemination and training (AGM Center Website) within a single framework. This allows researchers, practitioners, and policy stakeholders to share and review analytical results under the same assumptions and input data. Beyond simply providing an analysis tool, this structure is meaningful because it offers a shared research foundation and collaborative environment for Korean-style power-system analysis.

This report summarizes the current functions and structure of the KPG Platform and presents baseline comparison results for its major simulation functions. It also analyzes the characteristics and strengths of the KPG Platform through comparisons with existing power-system analysis and generation-scheduling tools, while reviewing its potential as an open-source platform for Korean power-system simulation and areas that still require improvement. The comparison tools selected in this report are Energy Exemplar's PLEXOS, Siemens' PSS/E, Argonne National Laboratory's UnitCommitment.jl, and Los Alamos National Laboratory's PowerModels.jl. The document is organized as follows.

- **Introduction to KPG TestGrid:** Summarizes the input data used in the comparison and the role of the test system.
- **Introduction to KPG Run:** Summarizes the core functions and representative formulations to clarify what kinds of problems are solved.
- **Structure of the comparison report:** Explains the reference tools, the comparison scope, and how the main text and appendix are organized.
- **Presentation of quantitative results:** Uses the comparison results to summarize the reliability of the KPG Platform and the implications for interpretation.

Version baseline. This comparison report was prepared as of March 2026 and is based on `KPG193 v1.5`, `KPG Run v1.0`, and `KPG View v1.0`. Some contents and results may change as the dataset and software are updated.

2. KPG Platform

2.1. KPG TestGrid

KPG TestGrid is an open test system that reflects the structural characteristics of the Korean power system, and a reduced 193-bus version called KPG 193 has currently been developed. Using publicly accessible data, KPG 193 represents 193 regional branch offices of the Korea Electric Power Corporation as buses and constructs a virtual transmission network for the year 2022. KPG 193 currently provides network location and facility information, generator commitment characteristics and cost parameters, and bus-level renewable generation capacities. It also provides hourly profiles of electricity demand, renewable generation, and weather data for all 8,760 hours of 2022. A technical description of KPG 193 is provided in the following reference [1].

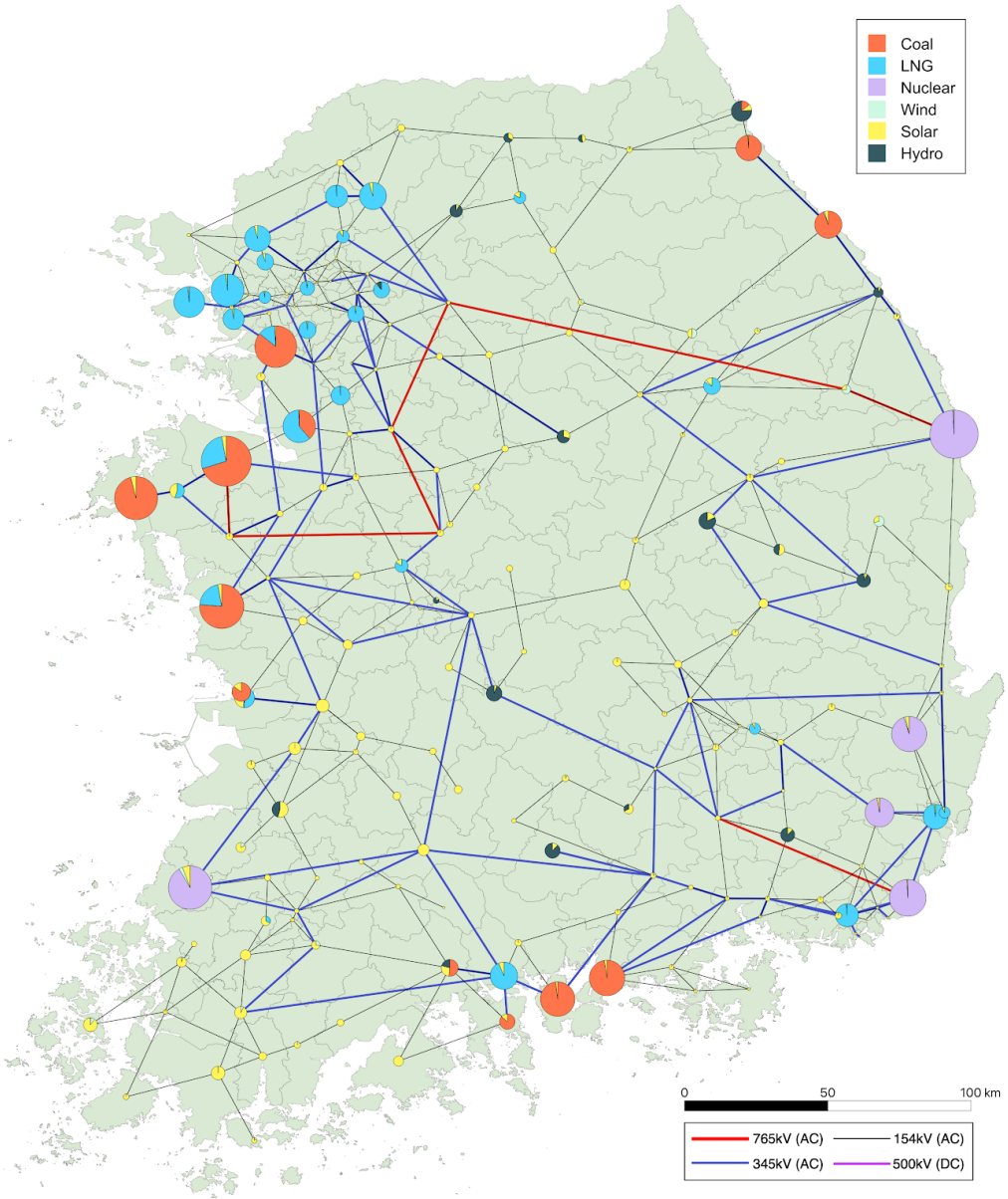

Figure 2. KPG 193 system topology

2.2. KPG Run

KPG Run is a generation-scheduling tool that takes either KPG TestGrid or a MATPOWER-format test system as input and solves unit commitment, economic dispatch, and AC/DC optimal power flow problems. The program is built in the Julia programming language, and users can simulate generation-scheduling problems through the interface shown in Figure 3 by selecting the problem type, target day, and solver engine.

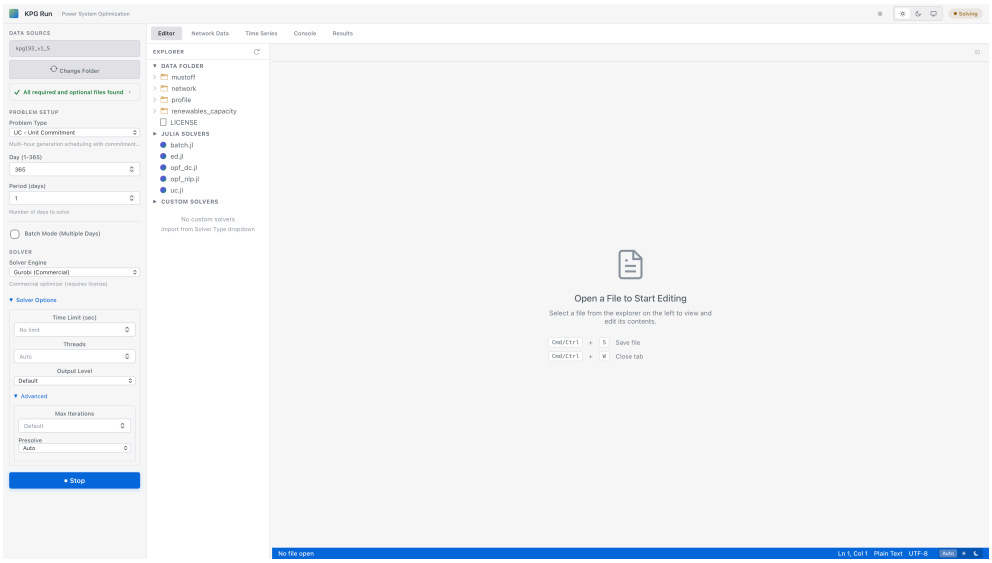

Figure 3. KPG Run user interface

Once a generation-scheduling problem has been solved in KPG Run, the interface moves to a results screen like the one shown in Figure 4. The results screen allows users to inspect generator operating points by hour and, in the case of optimal power flow, the line flows on the network. The solution outputs are saved both as `.csv` files and in a `.geojson` format that can be linked with KPG View.

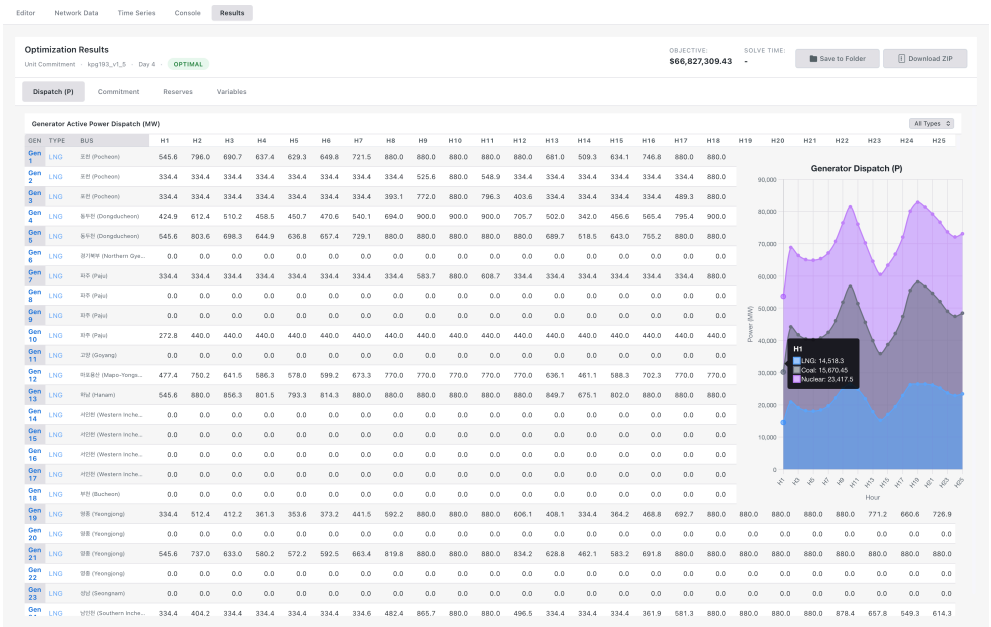

Figure 4. Example of the KPG Run results screen

Below, we summarize the formulations of UC, DCOPF, and ACOPF among the optimization problems implemented in KPG Run, as these are the formulations used in the comparison.

2.2.1. Notation

Symbol	Meaning
$\mathcal{I}, \mathcal{B}, \mathcal{L}, \mathcal{T}$	Sets of generators, buses, lines, and time periods, respectively
i, b, l, t	Indices for generators, buses, lines, and time, respectively
Ξ	Set of decision variables for each optimization problem
u_{it}, v_{it}, w_{it}	On/off status, start-up, and shut-down binary variables in UC
p_{it}, q_{it}	Active and reactive power output of generators
$r_{it}^{\mathsf{up}}, r_{it}^{\mathsf{dn}}$	Upward and downward reserves
θ_{bt}, v_{bt}	Bus voltage angle and voltage magnitude
p_{lt}^{ft}, p_{lt}^{tf}	Forward and reverse active power flow on line l
q_{lt}^{ft}, q_{lt}^{tf}	Forward and reverse reactive power flow on line l
$\underline{P}, \overline{P}, \underline{Q}, \overline{Q}$	Lower and upper bounds on active and reactive power output
$\overline{F}, \overline{\Delta}$	Upper bounds on line capacity and phase-angle difference
$C_i^g, \mathsf{C}_i^U, \mathsf{C}_i^D$	Generation, start-up, and shut-down cost functions
U_{it}	On/off status of a generator
$X_l, G_l, B_l, L_{l0}, L_{l1}$	Line reactance, conductance, susceptance, and DC loss coefficients

2.2.2. Direct Current Optimal Power Flow (DCOPF)

$$\min_{\Xi} \quad \sum_{i\in\mathcal{I}}\sum_{t\in\mathcal{T}} C_i^g(p_{it}) \tag{1}$$

$$\text{s.t.} \quad \underline{P}_i U_{it} \le p_{it} \le \overline{P}_i U_{it}, \tag{2}$$

$$-\overline{\Delta}_l \le \theta_{s(l),t} - \theta_{r(l),t} \le \overline{\Delta}_l, \quad \forall l \in \mathcal{L},\ t \in \mathcal{T}, \tag{3}$$

$$p_{lt}^{ft} = \frac{1}{X_l}(\theta_{s(l),t} - \theta_{r(l),t}), \quad \forall l \in \mathcal{L},\ t \in \mathcal{T}, \tag{4}$$

$$p_{lt}^{tf} = \frac{1}{X_l}(\theta_{r(l),t} - \theta_{s(l),t}), \quad \forall l \in \mathcal{L},\ t \in \mathcal{T}, \tag{5}$$

$$-\overline{F}_l \le p_{lt}^{ft} \le \overline{F}_l, \quad \forall l \in \mathcal{L},\ t \in \mathcal{T}, \tag{6}$$

$$-\overline{F}_l \le p_{lt}^{tf} \le \overline{F}_l, \quad \forall l \in \mathcal{L},\ t \in \mathcal{T}, \tag{7}$$

$$p_{lt}^{ft} - p_{lt}^{tf} = L_{l1} p_{lt}^{ft} + L_{l0}, \quad \forall l \in \mathcal{L}^{\mathsf{DC}},\ t \in \mathcal{T}, \tag{8}$$

$$P_{bt}^{d} - \sum_{l|s(l)=b} p_{lt}^{ft} - \sum_{l|r(l)=b} p_{lt}^{tf} = \sum_{i\in\mathcal{I}_b} p_{it}, \quad \forall b \in \mathcal{B},\ t \in \mathcal{T}. \tag{9}$$

where $\Xi = \{p_{it} \ge 0;\ |\theta_{bt}| \le \pi;\ p_{lt}^{ft}, p_{lt}^{tf} : \text{free}\}$.

2.2.3. Alternating Current Optimal Power Flow (ACOPF)

$$\min_{\Xi} \quad \sum_{i\in\mathcal{I}}\sum_{t\in\mathcal{T}} C_i^g(p_{it}) \tag{10}$$

$$\text{s.t.} \quad \underline{P}_i U_{it} \le p_{it} \le \overline{P}_i U_{it}, \quad \forall i \in \mathcal{I},\ t \in \mathcal{T}, \tag{11}$$

$$\underline{Q}_i U_{it} \le q_{it} \le \overline{Q}_i U_{it}, \quad \forall i \in \mathcal{I},\ t \in \mathcal{T}, \tag{12}$$

$$p_{lt}^{ft} = v_{s(l),t}\, v_{r(l),t}\big[G_l \cos(\theta_{s(l),t} - \theta_{r(l),t}) + B_l \sin(\theta_{s(l),t} - \theta_{r(l),t})\big], \quad \forall l \in \mathcal{L}^{\mathsf{AC}},\ t \in \mathcal{T}, \tag{13}$$

$$p_{lt}^{tf} = v_{r(l),t}\, v_{s(l),t}\big[G_l \cos(\theta_{r(l),t} - \theta_{s(l),t}) + B_l \sin(\theta_{r(l),t} - \theta_{s(l),t})\big], \quad \forall l \in \mathcal{L}^{\mathsf{AC}},\ t \in \mathcal{T} \tag{14}$$

$$q_{lt}^{ft} = v_{s(l),t}\, v_{r(l),t}\big[G_l \sin(\theta_{s(l),t} - \theta_{r(l),t}) - B_l \cos(\theta_{s(l),t} - \theta_{r(l),t})\big], \quad \forall l \in \mathcal{L}^{\mathsf{AC}},\ t \in \mathcal{T} \tag{15}$$

$$q_{lt}^{tf} = v_{r(l),t}\, v_{s(l),t}\big[G_l \sin(\theta_{r(l),t} - \theta_{s(l),t}) - B_l \cos(\theta_{r(l),t} - \theta_{s(l),t})\big], \quad \forall l \in \mathcal{L}^{\mathsf{AC}},\ t \in \mathcal{T} \tag{16}$$

$$(p_{lt}^{ft})^2 + (q_{lt}^{ft})^2 \le (\varepsilon_l\, A_l\, \overline{F}_l)^2, \quad \forall l \in \mathcal{L}^{\mathsf{AC}},\ t \in \mathcal{T} \tag{17}$$

$$(p_{lt}^{tf})^2 + (q_{lt}^{tf})^2 \le (\varepsilon_l\, A_l\, \overline{F}_l)^2, \quad \forall l \in \mathcal{L}^{\mathsf{AC}},\ t \in \mathcal{T} \tag{18}$$

$$-\Delta_l \le \theta_{s(l),t} - \theta_{r(l),t} \le \Delta_l, \quad \forall l \in \mathcal{L}^{\mathsf{AC}},\ t \in \mathcal{T} \tag{19}$$

$$p_{lt}^{ft} + p_{lt}^{tf} = L_d^0 + L_d^1\, p_{lt}^{ft}, \quad \forall l \in \mathcal{L}^{\mathsf{DC}},\ t \in \mathcal{T} \tag{20}$$

$$\underline{P}_l^{\mathsf{DC}} \le p_{lt}^{ft} \le \overline{P}_l^{\mathsf{DC}}, \quad \forall l \in \mathcal{L}^{\mathsf{DC}},\ t \in \mathcal{T} \tag{21}$$

$$\underline{P}_l^{\mathsf{DC}} \le p_{lt}^{tf} \le \overline{P}_l^{\mathsf{DC}}, \quad \forall l \in \mathcal{L}^{\mathsf{DC}},\ t \in \mathcal{T} \tag{22}$$

$$\underline{Q}_l^{\mathsf{DC}} \le q_{lt}^{ft} \le \overline{Q}_l^{\mathsf{DC}}, \quad \forall l \in \mathcal{L}^{\mathsf{DC}},\ t \in \mathcal{T} \tag{23}$$

$$\underline{Q}_l^{\mathsf{DC}} \le q_{lt}^{tf} \le \overline{Q}_l^{\mathsf{DC}}, \quad \forall l \in \mathcal{L}^{\mathsf{DC}},\ t \in \mathcal{T} \tag{24}$$

$$P_{bt}^D - \sum_{l\,:\,s(l)=b} p_{lt}^{ft} - \sum_{l\,:\,r(l)=b} p_{lt}^{tf} = \sum_{i\in\mathcal{I}_b} p_{it} \quad \forall b \in \mathcal{B},\ t \in \mathcal{T} \tag{25}$$

$$Q_{bt}^D - \sum_{l\,:\,s(l)=b} q_{lt}^{ft} - \sum_{l\,:\,r(l)=b} q_{lt}^{tf} = \sum_{i\in\mathcal{I}_b} q_{it}, \quad \forall b \in \mathcal{B}\ t \in \mathcal{T}. \tag{26}$$

where $\Xi = \{p_{it} \ge 0;\ 0.95 \le v_{bt} \le 1.05;\ |\theta_{bt}| \le \pi; q_{it}, p_{lt}^{ft}, p_{lt}^{tf}, q_{lt}^{ft}, q_{lt}^{tf}$: free$\}$.

2.2.4. Network-Constrained UC [2]

$$\min_{\Xi} \quad \sum_{i\in\mathcal{I}}\sum_{t\in\mathcal{T}}\Big(C_i^g(p_{it0}) + \mathsf{C}_i^U(v_{it0}) + \mathsf{C}_i^D(w_{it0})\Big) \tag{27}$$

$$\text{s.t.} \quad 0 \le r_{it}^{\mathsf{up}} \le \overline{R}_{it}^{\mathsf{up}} u_{it}, \tag{28}$$

$$0 \le r_{it}^{\mathsf{dn}} \le \overline{R}_{it}^{\mathsf{dn}} u_{it}, \tag{29}$$

$$p_{it} + r_{it}^{\mathsf{up}} \le (\overline{P}_i - \underline{P}_i)u_{it} - \big(\overline{P}_i - SU_i\big)\, v_{i,t}, \quad \forall i \in \mathcal{I},\, t \in \mathcal{T}, \tag{30}$$

$$p_{it} + r_{it}^{\mathsf{up}} \le (\overline{P}_i - \underline{P}_i)u_{it} - \big(\overline{P}_i - SD_i\big)\, w_{i,t+1}, \quad \forall i \in \mathcal{I},\, t \in \mathcal{T}, \tag{31}$$

$$p_{it} + r_{it}^{\mathsf{up}} - p_{i,t-1} \le P_i^{\mathsf{RU}}, \quad \forall i \in \mathcal{I},\, t \in \mathcal{T}, \tag{32}$$

$$p_{i,t-1} - (p_{it} - r_{it}^{\mathsf{dn}}) \le P_i^{\mathsf{RD}}, \quad \forall i \in \mathcal{I},\, t \in \mathcal{T}, \tag{33}$$

$$p_{it}^{\mathsf{G}} = \underline{P}_i u_{it} + p_{it}, \quad \forall i \in \mathcal{I},\, t \in \mathcal{T}, \tag{34}$$

$$\sum_{\tau=t-UT_i+1}^{t} v_{i\tau} \le u_{it}, \quad \forall i \in \mathcal{I},\, t \in \mathcal{T}, \tag{35}$$

$$\sum_{\tau=t-DT_i+1}^{t} w_{i\tau} \le 1 - u_{it}, \quad \forall i \in \mathcal{I},\, t \in \mathcal{T}, \tag{36}$$

$$u_{it} - u_{i,t-1} = v_{it} - w_{it}, \quad \forall i \in \mathcal{I},\, t \in \mathcal{T}, \tag{37}$$

$$-\overline{\Delta}_l \le \theta_{s(l),t} - \theta_{r(l),t} \le \overline{\Delta}_l, \quad \forall l \in \mathcal{L},\, t \in \mathcal{T}, \tag{38}$$

$$p_{lt}^{ft} = \frac{1}{X_l}(\theta_{s(l),t} - \theta_{r(l),t}), \quad \forall l \in \mathcal{L},\, t \in \mathcal{T}, \tag{39}$$

$$p_{lt}^{tf} = \frac{1}{X_l}(\theta_{r(l),t} - \theta_{s(l),t}), \quad \forall l \in \mathcal{L},\, t \in \mathcal{T}, \tag{40}$$

$$-\overline{F}_l \le p_{lt}^{ft} \le \overline{F}_l, \quad \forall l \in \mathcal{L},\, t \in \mathcal{T}, \tag{41}$$

$$-\overline{F}_l \le p_{lt}^{tf} \le \overline{F}_l, \quad \forall l \in \mathcal{L},\, t \in \mathcal{T}, \tag{42}$$

$$p_{lt}^{ft} - p_{lt}^{tf} = L_{l1}p_{lt}^{ft} + L_{l0}, \quad \forall l \in \mathcal{L}^{\mathsf{DC}},\, t \in \mathcal{T}, \tag{43}$$

$$P_{bt}^{d} - \sum_{l|s(l)=b} p_{lt}^{ft} - \sum_{l|r(l)=b} p_{lt}^{tf} = \sum_{i\in\mathcal{I}_b} p_{it}, \quad \forall b \in \mathcal{B},\, t \in \mathcal{T}. \tag{44}$$

where $\Xi = \{u_{it}, y_{it}, z_{it} \in \{0,1\};\ p_{it}, r_{it}^{+}, r_{it}^{-} \ge 0;\ |\theta_{bt}| \le \pi;\ p_{lt}^{ft}, p_{lt}^{tf} : \text{free}\}$.

3. Structure and Scope of the Comparison Report

The previous section summarized the components of the KPG Platform, especially the roles of KPG TestGrid and KPG Run. This section explains the comparison framework and scope adopted in this report.

3.1. Comparison Targets and Objectives

To compare the calculation results of KPG Run, this report selects the commercial tools PLEXOS and PSS/E and the open-source tools UnitCommitment.jl and PowerModels.jl as reference tools. The selection criteria were the level of practical use of each tool and its suitability for specific optimization problem types.

Tool	Type	Description
PLEXOS	Commercial	A widely used commercial tool for power-system planning and operations analysis, used here to compare KPG Run's UC results against a benchmark familiar in practice
PSS/E	Commercial	A widely used commercial tool for transmission power-flow calculation and system analysis, used here to compare KPG Run's ACOPF results against commercial analysis results
UnitCommitment.jl	Open-source	An open UC optimization package whose formulation and implementation can be directly inspected, used here to compare KPG Run's UC results in a reproducible manner[1]
PowerModels.jl	Open-source	An open package that provides multiple network-optimization formulations, used here to compare KPG Run's DCOPF and ACOPF results against reproducible reference results[2]

Table 2. Reference tools used in this report

This report compares KPG Run's calculation results against both commercial tools and open-source tools. Commercial tools serve as a benchmark for consistency with analysis results widely used in practice, while open-source tools provide a transparent and reproducible basis because their formulations and computational settings can be tracked directly. Accordingly, the primary objective of this report is to demonstrate the technical reliability of the KPG Platform by comparing its numerical results with trusted commercial and open-source tools. A secondary objective is to document the differences observed during the comparison process so that they can serve as reference material for future development and follow-up comparison work.

The comparison covers the UC, DCOPF, ACOPF, and ACPF functions of KPG Run. The main text presents the representative Day 1–90 results, while the remaining Day 1–365 results are organized in the appendix. The comparison scope for each function is as follows.

Comparison model	Comparison target
ACPF	PSS/E
DCOPF	PowerModels.jl
ACOPF	PowerModels.jl
UC	PLEXOS, UnitCommitment.jl

Table 3. Scope of the comparison report

4. Comparison with Open-Source Reference Tools

This section first presents the comparison results against reproducible open-source reference tools. The main text reports the representative Day 1–90 interval, while the Day 1–365 long-horizon aggregates and quarterly figures are collected in Appendix A.

4.1. Summary

Problem type	Reference tool	Period	Summary
UC	UnitCommitment.jl	Day 1–90	Mean absolute objective difference of 0.0447% and mean status mismatch rate of 1.17%
DCOPF	PowerModels.jl	Day 1–90	No absolute objective difference observed
ACOPF	PowerModels.jl	Day 1–90	Mean absolute objective difference of about 0.0303%

Table 4. Summary of comparisons with open-source reference tools for Day 1–90

4.2. UC: KPG Run vs UnitCommitment.jl

The UC comparison examines both the objective value and generator on/off status. The main text uses the Day 1–90 results, and status mismatch is summarized as the fraction of mismatched points out of the daily total of 2928 comparison points, corresponding to 24 hourly states for each of 122 generators.

Metric	Value
Comparison period	Day 1–90
Number of status comparisons per day (122 units $\times$ 24 hours)	2928
Mean absolute objective difference (%)	0.0447
Maximum absolute objective difference (%)	0.255 (Day 1)
Mean status mismatch rate (%)	1.17
Day with maximum status mismatch	Day 65 (3.96%)

Table 5. Summary of absolute UC objective differences and status mismatch for Day 1–90

Over the representative 90-day interval, the mean absolute objective difference is small at 0.0447%, and the status mismatch rate also remains low. The Day 1–365 aggregate statistics and quarterly figures are provided in Appendix A.

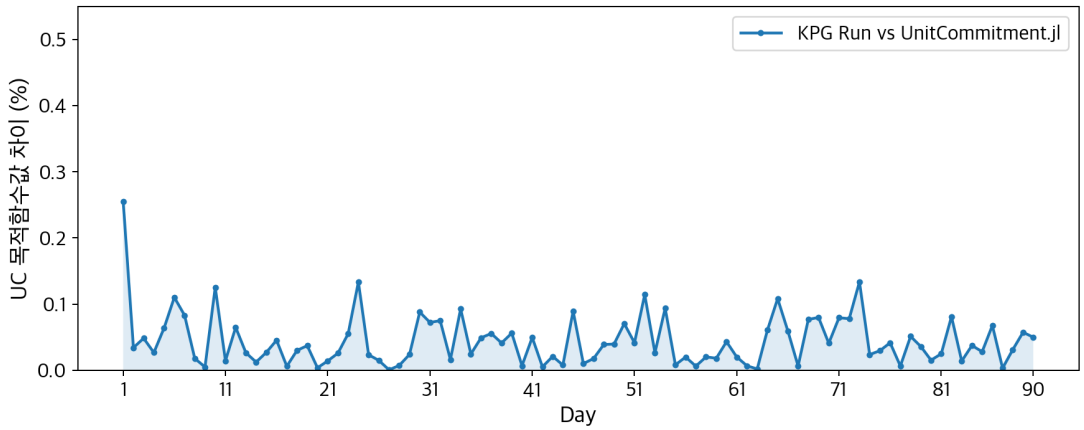

Figure 5. Absolute UC objective difference relative to UnitCommitment.jl for Day 1–90

Reason for the difference. UnitCommitment.jl is a reference tool for computing network-constrained UC, but it does not include HVDC line modeling. Accordingly, differences in the objective value and generator status arise when it is compared against KPG Run, which includes HVDC line modeling.

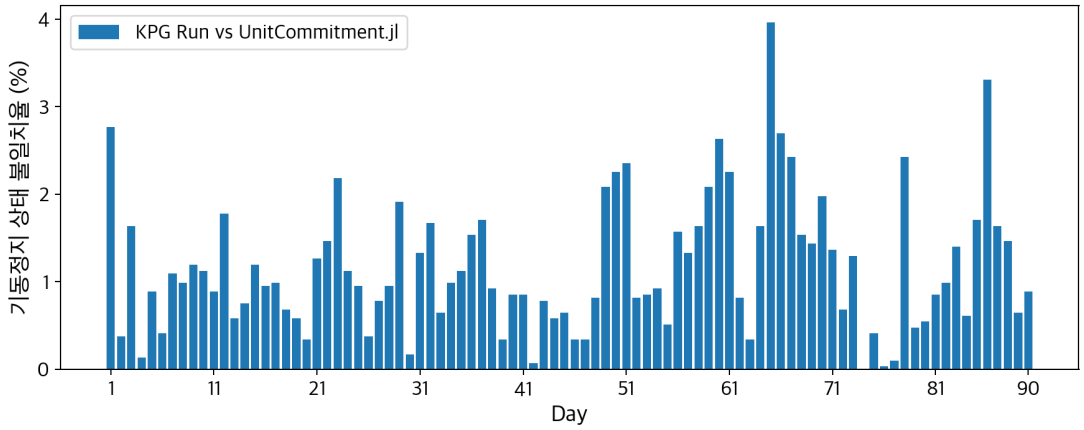

Figure 6. UC status mismatch rate relative to UnitCommitment.jl for Day 1–90

4.3. DCOPF: KPG Run vs PowerModels.jl

The DCOPF comparison is summarized using the objective value. The main text uses the Day 1–90 results and reports the absolute objective difference.

Metric	Value
Comparison period	Day 1–90
Mean absolute objective difference (%)	0.0
Maximum absolute objective difference (%)	0.0

Table 6. Summary of DCOPF objective differences for Day 1–90

No absolute objective difference was observed over Day 1–90. In other words, within the scope of this comparison, the DCOPF objective values of KPG Run and PowerModels.jl were identical.

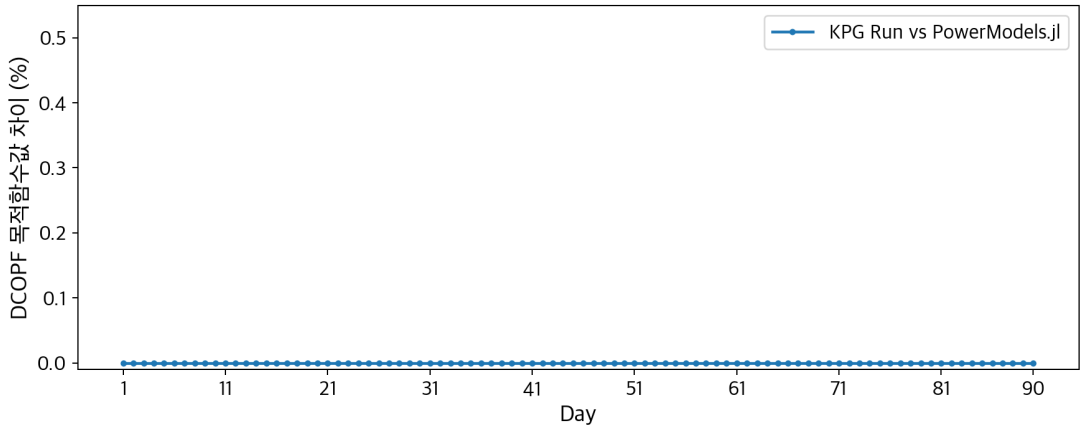

Figure 7. Absolute DCOPF objective difference relative to PowerModels.jl for Day 1–90

4.4. ACOPF: KPG Run vs PowerModels.jl

The ACOPF comparison is summarized using the objective value. The main text uses the Day 1–90 results and reports the absolute objective difference.

Metric	Value
Comparison period	Day 1–90
Mean absolute objective difference (%)	0.0303
Maximum absolute objective difference (%)	0.105 (Day 29)

Table 7. Summary of ACOPF objective differences for Day 1–90

Over Day 1–90, the mean absolute objective difference is 0.0303%, and the maximum absolute error is 0.105% on Day 29. The difference is larger than in DCOPF, but it remains small even after accounting for nonlinearity and solver tolerances.

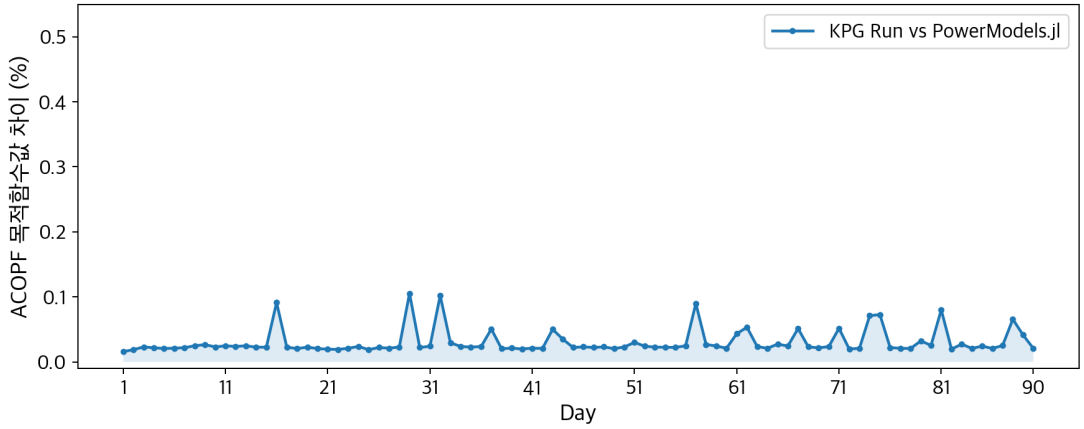

Figure 8. Absolute ACOPF objective difference relative to PowerModels.jl for Day 1–90

5. Comparison with Commercial Software

After confirming strong consistency in the comparison with open-source reference tools, this section presents the comparison results against commercial benchmark tools. The main text contains the representative Day 1–90 interval, while the Day 1–365 results for PLEXOS and PSS/E are collected in Appendix A.

5.1. UC: KPG Run vs PLEXOS

The PLEXOS nodal UC export generated the final solution file throughout the long-horizon comparison period. This indicates that the PLEXOS model completed the long-horizon simulation stably under the given conditions. Among those results, the Day 1–90 interval is directly compared with the raw UC results of KPG Run to present the key quantitative indicators.

PLEXOS and KPG Run differ in how UC is constructed. In particular, they do not treat the carry-over of previous-day operating states or the implementation of minimum up-time and minimum down-time constraints in the same way. For this reason, PLEXOS results are useful as a benchmark for verifying whether long-horizon simulations can be completed stably, but they are limited as a direct benchmark for continuous generation-scheduling results against KPG Run. Accordingly, the state and dispatch differences shown here should be interpreted as consequences of differences in modeling conditions rather than calculation failure. From the perspective of continuous generation scheduling, KPG Run is the more direct reference.

Even over Day 1–90, both the status mismatch rate and dispatch MAE remain persistently high. This is interpreted as a structural divergence in the commitment path caused by the different ways in which

Metric	Value
Long-horizon comparison scope	Day 1–365
Quantitative comparison scope in the main text	Day 1–90 (90 days)
Mean status mismatch rate (%)	28.1
Maximum status mismatch rate (%)	39.38 (Day 33)
Mean dispatch MAE (MW)	207.7
Maximum dispatch MAE (MW)	230.0 (Day 72)

Table 8. Summary of the PLEXOS vs KPG Run UC comparison for Day 1–90

previous-day operating states and minimum up/down times are represented. The full 365-day direct-comparison summary is provided in Appendix A.

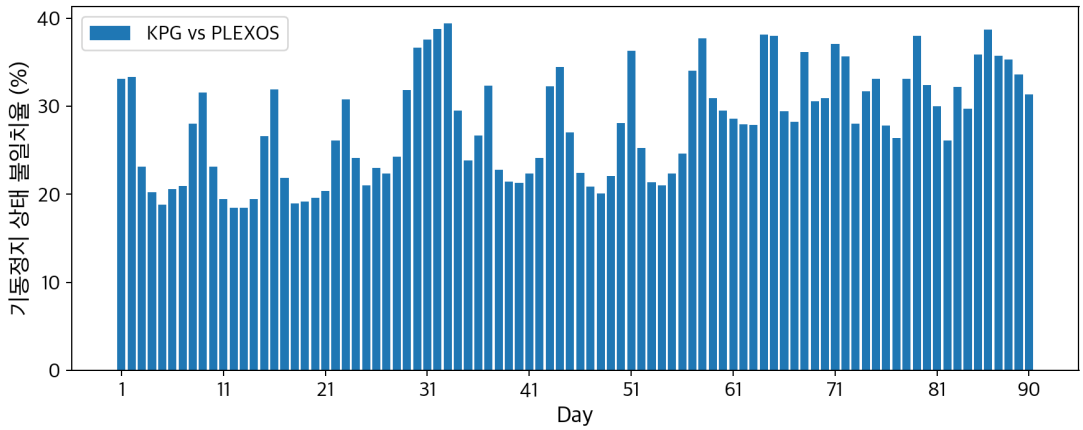

Figure 9. Daily status mismatch rate of KPG Run relative to PLEXOS for Day 1–90

Reason for the difference. PLEXOS and KPG Run differ in how they carry over previous-day operating states and how they implement minimum up-time and minimum down-time constraints. Therefore, the status mismatch can be interpreted as a consequence of differences in modeling conditions.

5.2. ACOPF: KPG Run vs PSS/E

In the PSS/E comparison, the ACOPF solution obtained from KPG Run was used to align the same initial conditions, after which power-flow analysis was performed in PSS/E and compared against the power-flow results of KPG Run. The main text presents the representative Day 1–90 interval, while the long-horizon results are organized in Appendix A.

The comparison is divided into two cases according to the HVDC treatment. Here, `equiv_load` denotes the case in which the terminal P/Q values of the HVDC line are injected as equivalent bus loads, whereas `native` denotes the case in which the PSS/E two-terminal DC line model is used directly.

In **Table 9**, max $|dV|$ denotes the maximum bus-voltage error observed during the day, max $|dP|$ denotes the maximum branch active-power error, and loss delta denotes the difference in total transmission losses.

Mode	Avg max $\lvert dV\rvert$	Avg max $\lvert dP\rvert$	Loss delta
`equiv_load`	2.27×10^{-7} pu	3.66×10^{-3} MW	-1.62×10^{-4} MW
`native`	5.29×10^{-2} pu	1.66×10^{3} MW	50.76 MW

Table 9. Summary of PSS/E mismatch analysis for Day 1–90

The Day 1–90 results show that when the simplified HVDC representation is applied, the power-flow results of KPG Run and PSS/E align very closely. By contrast, once the more detailed HVDC model is

used, the differences become clearly larger. This suggests that planning-oriented ACOPF and system-analysis-oriented PSS/E should not be forced into a strict one-to-one benchmark relationship, but rather understood as analysis tools designed for different purposes.

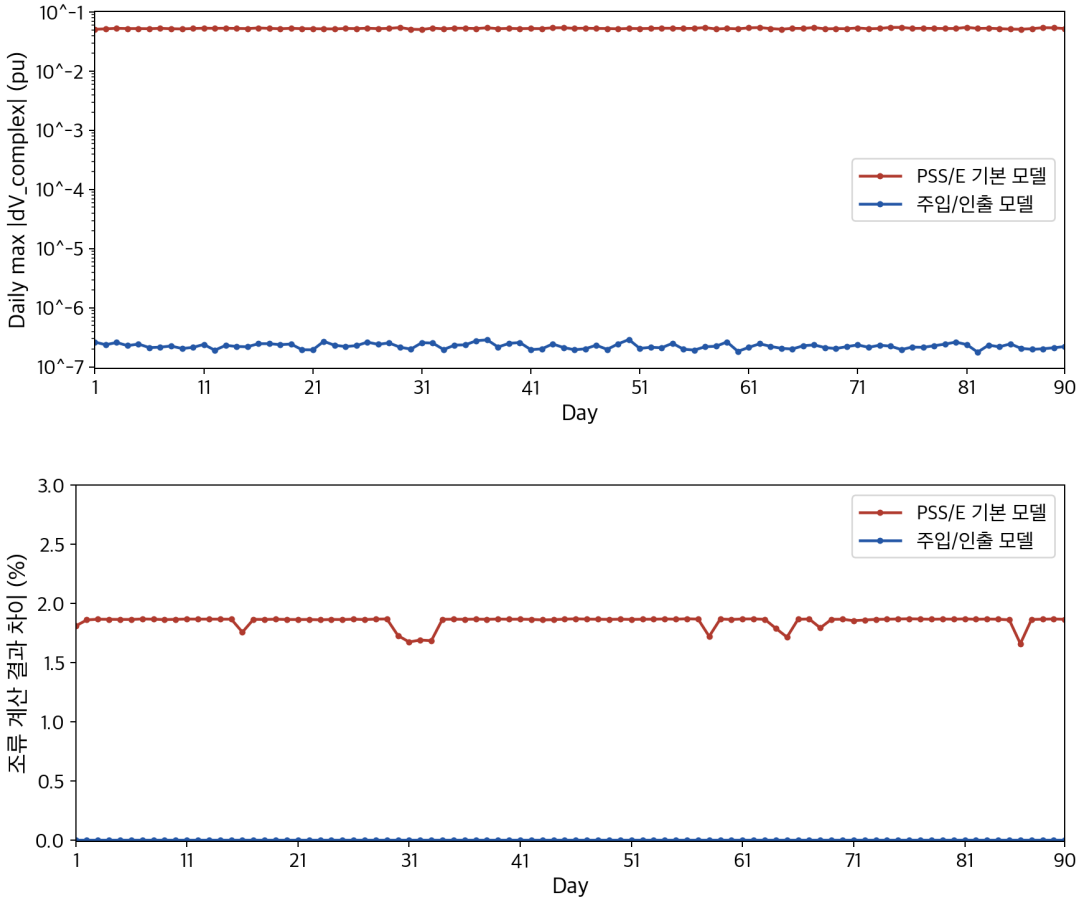

Figure 10. Voltage mismatch and mean branch-flow error rate (%) of KPG Run relative to PSS/E for Day 1–90 (log scale)

6. Conclusions and Future Development Directions

This report presented the representative Day 1–90 results in the main text and included the Day 1–365 long-horizon aggregates in the appendix. Based on these materials, it organized both the quantitative comparisons and the interpretive basis for the UC, DCOPF, and ACOPF results of KPG Run. The comparison with open-source reference tools confirmed a high level of numerical consistency overall, while the comparison with commercial tools highlighted the impact of differences in modeling approaches and simulation conditions.

The PSS/E results showed strong consistency with KPG Run when a simplified HVDC representation was used, but the differences widened when a more detailed model was applied. This suggests that planning-oriented ACOPF and system-analysis-oriented PSS/E should be interpreted as tools with different purposes rather than evaluated under exactly the same standard. In future development of KPG Run, it will be necessary to find a balance between preserving tractability as a generation-scheduling model and achieving the level of detail required from a system-analysis perspective.

The PLEXOS results did not directly match KPG Run because of differences in initial-state linkage and simulation conditions. However, PLEXOS has the characteristic that daily simulations can be performed relatively independently, in contrast to the KPG Run UC workflow, which requires information from the

previous day. This indicates that future development of KPG Run should preserve the accuracy of state linkage while also considering a more flexible execution structure from the standpoint of repeated simulation and user operation.

A. Full-Period Results and Detailed Analysis

This appendix organizes the long-horizon aggregates and representative-case analyses corresponding to the results summarized in the main text. The long-horizon comparison scope is uniformly defined as Day 1–365, and detailed metrics and representative examples are presented for each comparison target. The long-horizon comparison checks whether the patterns observed in the 90-day representative interval of the main text remain valid across changing seasons and load levels.

A.1. Open-Source Results for the Full Period

Problem type	Period	Full-period summary
UC	Day 1–365	Mean absolute objective difference of 0.0537%, mean status mismatch rate of 1.20%, and worst day on Day 65 (3.96%)
DCOPF	Day 1–365	No absolute objective difference observed over the full period
ACOPF	Day 1–365	Mean absolute objective difference of 0.0366%, with the maximum absolute error of 0.328% on Day 134

Table 10. Summary of comparisons with open-source reference tools over the full period

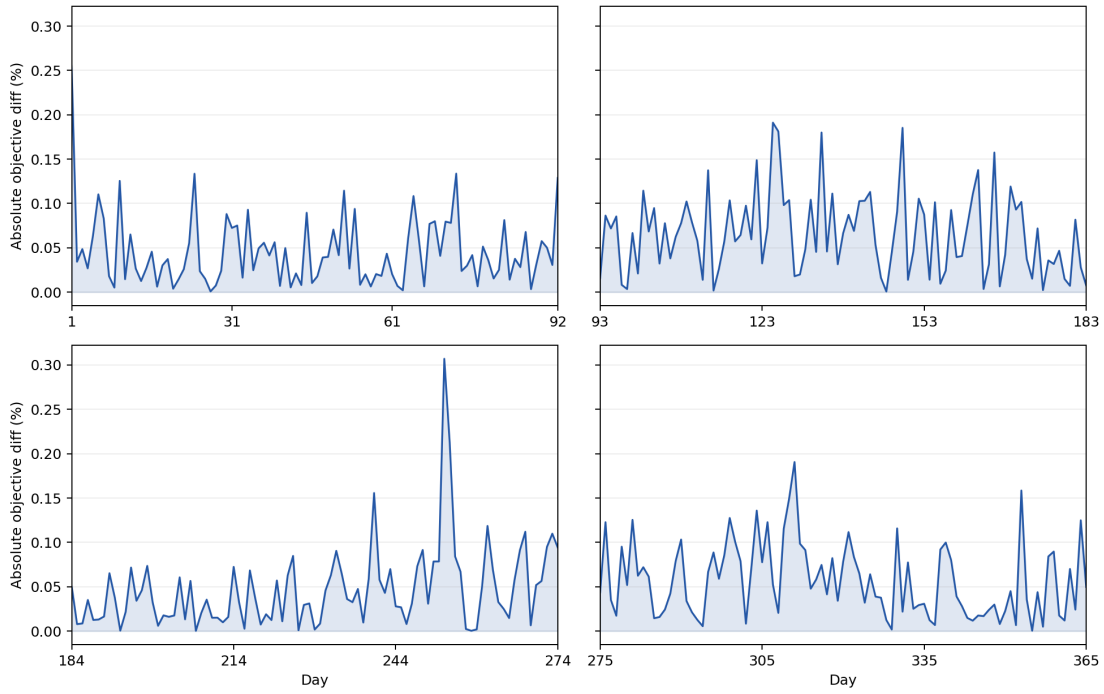

Figure 11. Quarterly plots of the absolute UC objective difference relative to UnitCommitment.jl over the full period

The conclusions observed in the representative 90-day interval of the main text remain unchanged in the long-horizon comparison results.

A.2. PLEXOS UC Results for the Full Period

The conclusions observed in the representative 90-day interval of the main text remain unchanged in the long-horizon comparison results.

A.3. PSS/E Results for the Full Period

`equiv_load` denotes the case in which the terminal P/Q values of the HVDC line are injected as equivalent bus loads, whereas `native` denotes the case in which the PSS/E two-terminal DC line model is used directly. max $|dV|$ denotes the maximum bus-voltage error, max $|dP|$ denotes the maximum branch active-power error, and loss delta denotes the difference in total losses.

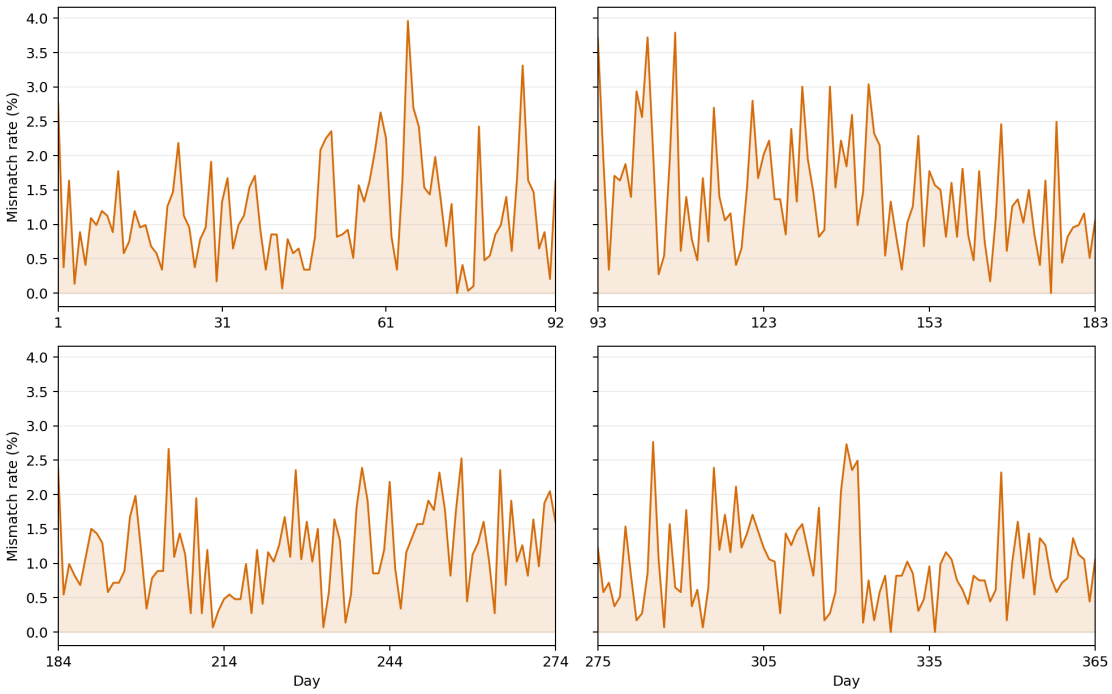

Figure 12. Quarterly plots of the UC status mismatch rate relative to UnitCommitment.jl over the full period

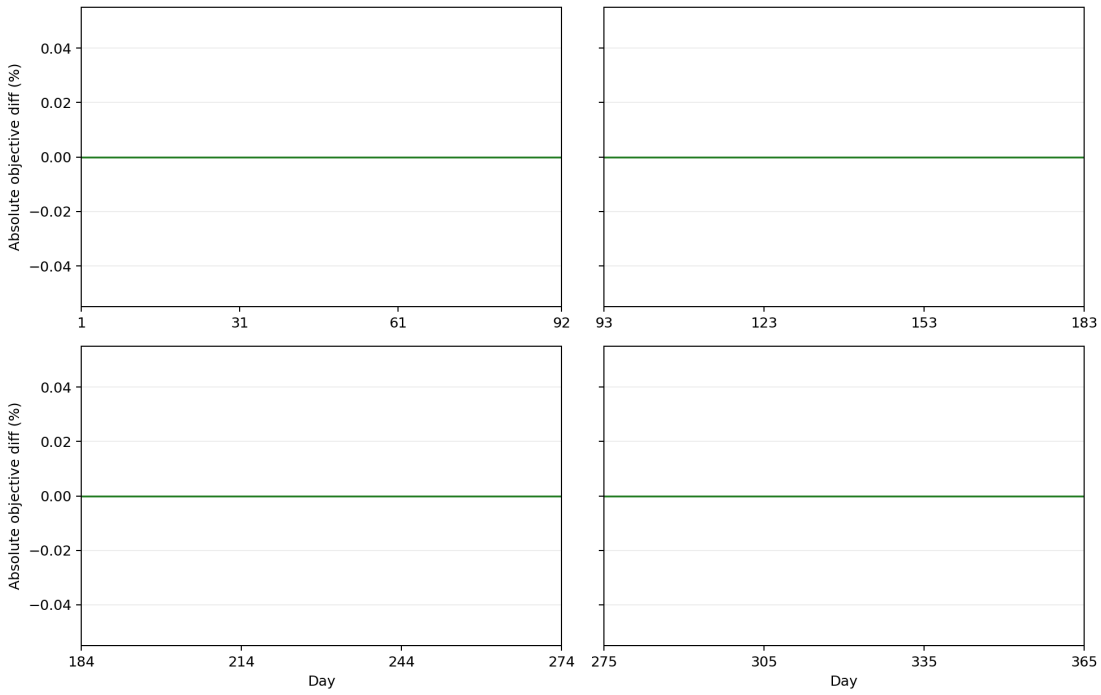

Figure 13. Quarterly plots of the absolute DCOPF objective difference relative to PowerModels.jl over the full period

Metric	Value
Long-horizon comparison scope	Day 1–365
Mean status mismatch rate (%)	31.0
Maximum status mismatch rate (%)	44.74 (Day 148)
Mean dispatch MAE (MW)	211.0
Maximum dispatch MAE (MW)	234.5 (Day 148)

Table 11. Summary of the PLEXOS vs KPG Run UC comparison over the full period

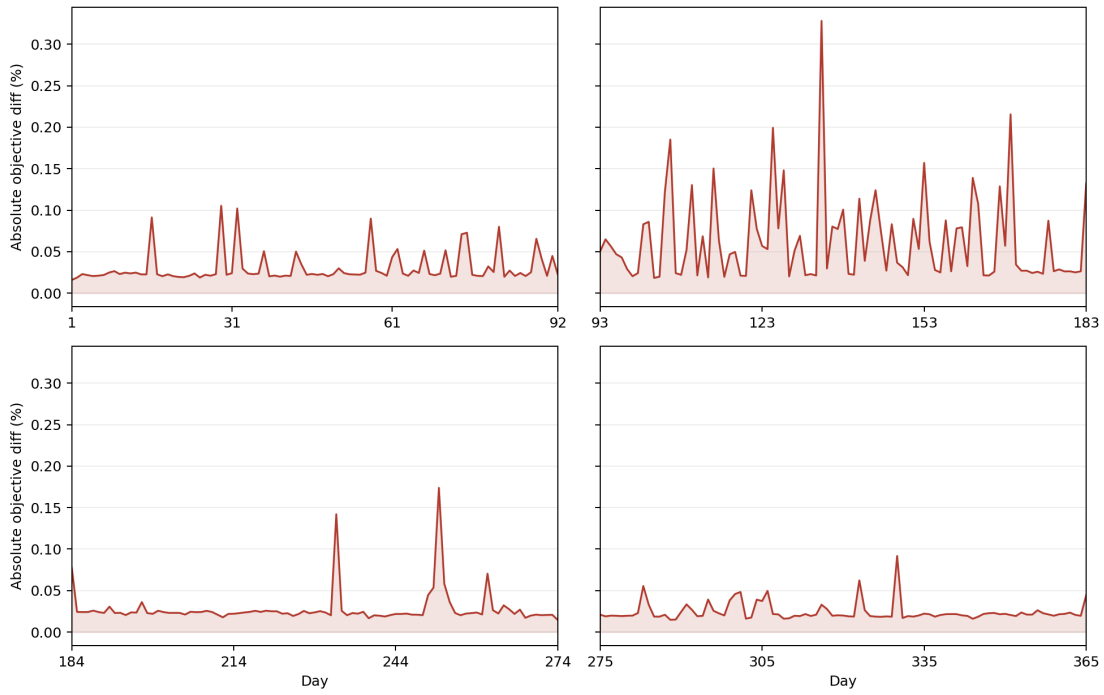

Figure 14. Quarterly plots of the absolute ACOPF objective difference relative to PowerModels.jl over the full period

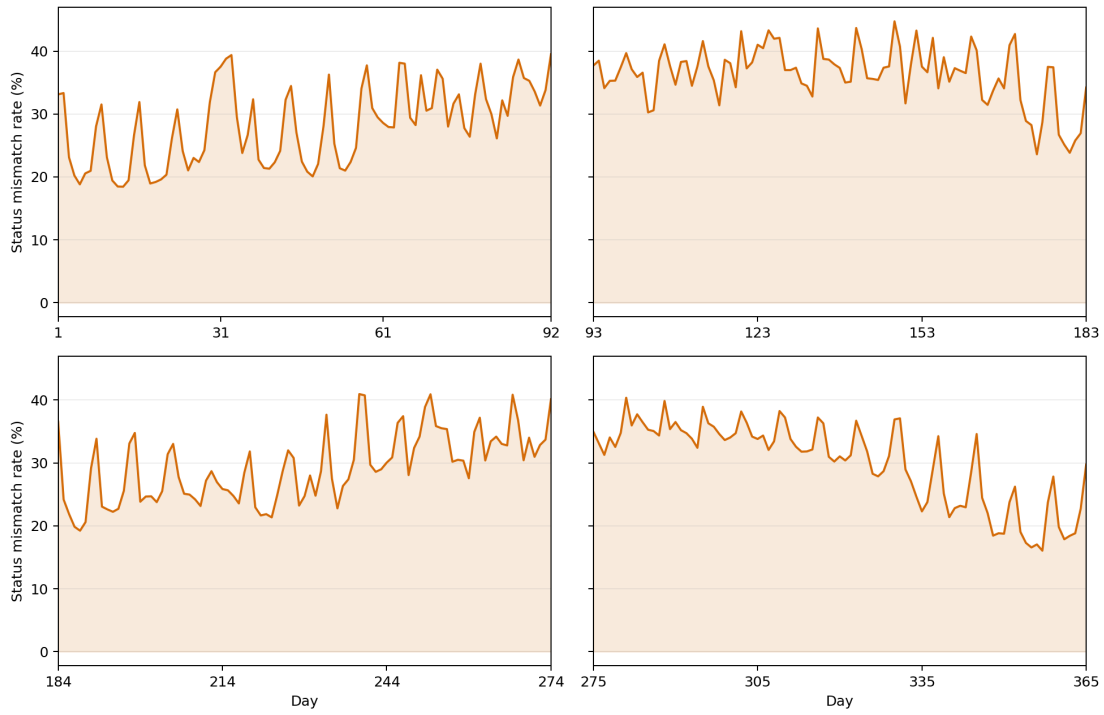

Figure 15. Quarterly plots of the status mismatch rate of KPG Run relative to PLEXOS over the full period

Mode	Avg max $\lvert dV \rvert$	Avg max $\lvert dP \rvert$	Loss delta
`equiv_load`	2.21×10^{-7} pu	3.64×10^{-3} MW	-1.40×10^{-4} MW
`native`	5.26×10^{-2} pu	1.66×10^{3} MW	46.88 MW

Table 12. Summary of PSS/E mismatch analysis over the full period

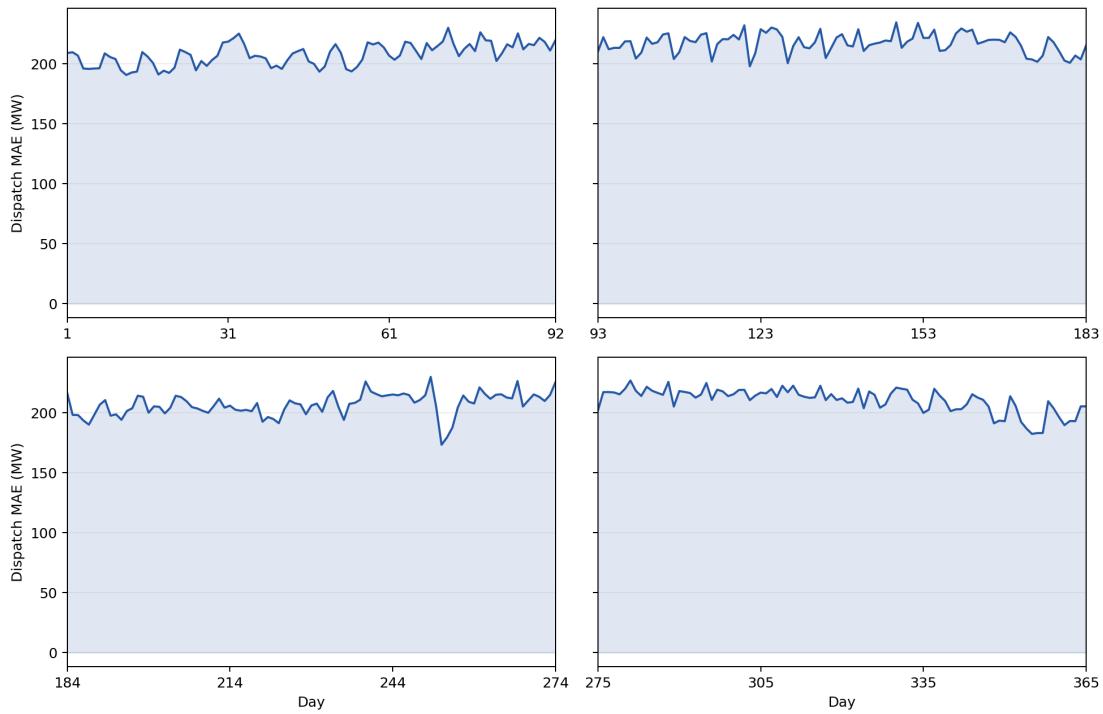

Figure 16. Quarterly plots of the dispatch MAE of KPG Run relative to PLEXOS over the full period

Over the full period as well, KPG Run and PSS/E produced very similar power-flow results when the simplified HVDC representation was used. By contrast, the differences expanded substantially when the more detailed HVDC model was applied.

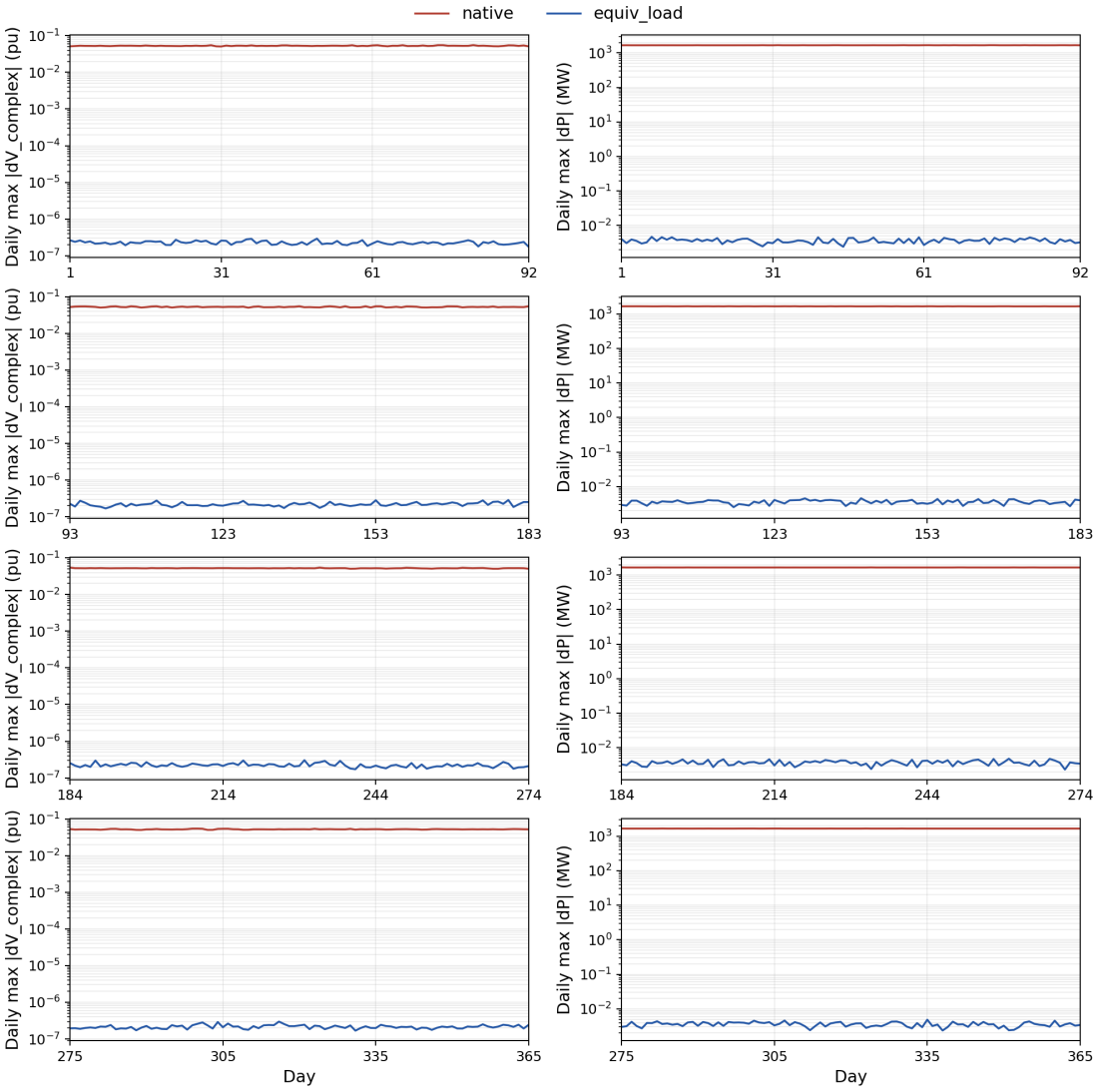

Figure 17. Quarterly comparison of KPG Run voltage and branch-flow mismatch relative to PSS/E over the full period (log scale)

References

[1] G. Song and J. Kim, “Kpg 193: A synthetic korean power grid test system for decarbonization studies,” *arXiv preprint arXiv:2411.14756*, 2024. [Online]. Available: https://arxiv.org/abs/2411.14756.

[2] G. Morales-España, J. M. Latorre, and A. Ramos, “Tight and compact milp formulation for the thermal unit commitment problem,” *IEEE Transactions on Power Systems*, vol. 28, no. 4, pp. 4897–4908, 2013.

[3] A. S. Xavier, A. M. Kazachkov, O. Yurdakul, J. He, and F. Qiu, *Unitcommitment.jl: A julia/jump optimization package for security-constrained unit commitment*, version 0.4, 2024. [Online]. Available: https://doi.org/10.5281/zenodo.4269874.

[4] C. Coffrin, R. Bent, K. Sundar, Y. Ng, and M. Lubin, “Powermodels.jl: An open-source framework for exploring power flow formulations,” in *Power Systems Computation Conference (PSCC)*, 2018. [Online]. Available: https://www.coffrin.com/publication/powermodels/.